Effects of water on pyridine pyrolysis: A reactive force field molecular dynamics study

Zhongze Bai [a], Xi Zhuo Jiang [b,**], Kai H. Luo [a,*]

[a] Department of Mechanical Engineering, University College London, Torrington Place, London, WC1E 7JE, UK
[b] School of Mechanical Engineering and Automation, Northeastern University, Shenyang, Liaoning, 110819, PR China

ARTICLE INFO

ABSTRACT

The emission of nitrogen oxides (NOx) from coal combustion causes serious environmental problems. Fuel splitting and staging is a promising method for NOx control by combustion modification. In this process, nitrogen-containing compounds generated from pyrolysis gas play an important role in regulating NOx generation. Water from coal could potentially change reactions during the coal pyrolysis process. Adjusting the content of water in coal may be an effective way to control coal pyrolysis reactions. This work aims to investigate the effects of water on pyridine (a main nitrogen-containing compound in coal) pyrolysis via reactive force field (ReaxFF) molecular dynamics (MD) simulations. Results indicate that the addition of water during the pyridine pyrolysis process increases the number of OH radicals in the system and accelerates the consumption of pyridine at the initial stage. However, at a later stage, water inhibits the consumption of pyridine as it impedes the condensation reaction of pyridine molecules. Common and unique intermediates are identified and quantified under various water-content conditions. Results suggest that water also reduces the proportion of nitrogen atoms in the poly-condensation product. Furthermore, ring opening processes of pyridine molecules are reproduced at the atomic level. The changes in reaction pathways due to the presence of water are also revealed. The new insights into the mechanisms of pyridine pyrolysis under water and water-free conditions provide a possibility to control nitrogen migration during the pyrolysis process, which is of great significance to emission reduction from coal combustion.

Credit author statement

1. Introduction

The emission of nitrogen oxides (NOx) from coal combustion causes serious environmental problems, such as photochemical smog and acid rain [1]. In recent years, a variety of technologies have been developed for coal combustion to control NOx emissions.

Fuel staging or reburning is a promising method for NOx control by combustion modification. The idea of fuel reburning is to recycle the NOx formed to nitrogen during combustion. The reburning reactor includes three zones [2]: a main reaction zone, where coal combustion under fuel-lean conditions takes place and NOx is generated, a reburning zone, where reburn fuel is injected and reacts with NOx forming N_2, a burnout zone, where air is added to ensure complete combustion of fuel.

Reburning fuels play a key role in NOx reduction during coal combustion. They can be divided into two categories: fossil fuels (such as natural gas, coal and oil) and pyrolysis gas. It is reported that pyrolysis gas has better performance in NOx reduction than fossil fuels [3–5]. In a fuel staging (also termed fuel splitting and staging) process, coal is decomposed to pyrolysis gas and char. Char and pyrolysis gas are primary fuel and reburning fuel respectively. Previous studies [3–5] have identified that the nitrogen-containing compounds in pyrolysis gas is important for effective NOx reduction in the fuel splitting and staging process. Water, an intrinsic component in coal, can accelerate coal pyrolysis process and greatly

alter products distribution in pyrolysis gas [6]. Therefore, adjusting the content of water in coal could be an effective way to control the N migration during coal pyrolysis, which has the potential to improve the NOx control performance during coal combustion.

Previous studies have explored chemical effects of water during coal pyrolysis by experiments and simulations. Ouyang and co-workers carried out experiments focusing on the effects of H_2O during char pyrolysis [7]. They proposed that H_2O reduced the char generation, stabilized the char structure and increased the char reaction rate. Hu and co-workers investigated the effects of H_2O on the pyrolysis of coal [8]. Results showed that the yield of tar and light tar decreased with water content increasing during the coal pyrolysis. Liu and co-workers interrogated pyrrole pyrolysis with water using a density functional theory method [9]. The computational research suggested that H_2O molecules inhibited the formation HCN but promoted the generation of NH_3. Gou and co-workers explored the effects of water vapor on the pyrolysis products of coal [6]. They found that water promoted the generation of HCN, NH_3, H_2 and CO, which can restrain the NOx formation during coal combustion [6]. Previous studies have made great contributions to understanding the pyrolysis phenomena from a wide range of perspectives, like the composition of products and reaction rate. However, there are some fundamental questions remaining unanswered. For example, the effects of water on the mechanisms of nitrogen-containing compounds pyrolysis in coal are still poorly understood. Further efforts are required to explore the atomic/molecular events therein and reveal the reaction mechanisms.

The current experimental techniques are unable to accurately detect the temporal evolution of the distributions of intermediates and products. Atomistic-scale computational techniques, like reactive molecular dynamics that can capture atomistic behaviors of constitutive atoms/molecules [10], lend the possibility to reveal the detailed reaction mechanisms and obtain intermediate structures [11,12] that cannot be obtained by current measurement methods. Among the existing atomistic methods, the ReaxFF MD is a promising method to simulate complex chemical reactions with reasonable computational cost and high accuracy. Recently, ReaxFF MD simulations have been applied to pyrolysis of coal [13–19] and chemical reactions of nitrogen-containing compounds [20,21]. However, due to the complexity and uncertainty of coal molecular structures, low content of nitrogen, and the influence of other radicals or functional groups [22], it is difficult to build a complete coal molecular model to investigate nitrogen properties during coal pyrolysis. Alternatively, nitrogen-containing compounds in coal such as pyridine [23,24] are used as a surrogate for coal.

In this study, a series of ReaxFF MD simulations are conducted to investigated the effects of water on pyridine pyrolysis. Firstly, effects of water on the pyridine pyrolysis rate and intermediates are studied. Secondly, ring-opening reactions and proportion of poly-condensation products are explored during pyrolysis. Finally, reaction mechanisms of principal products like H_2, CO, HCN and NH_3 are compared between conditions with and without water addition.

2. Methods

2.1. ReaxFF MD

The ReaxFF is a force field MD method that lies in between quantum chemical simulation and classical molecular dynamics simulation, which was originally developed by van Duin and co-workers [25] to study the kinetics of chemical reactions. ReaxFF employs a bond-order formalism in conjunction with polarizable charge descriptions to determine both reactive and non-reactive

interactions between atoms [26]. Energy contributions to the ReaxFF potential are shown in Equation (1):

$$E_{system} = E_{bond} + E_{over} + E_{angle} + E_{tors} + E_{vdWaals} + E_{Coulomb} + E_{Specific} \quad (1)$$

where the terms are total energy, bond energy, penalty energy, valence angle energy, torsion angle energy, van der Waals energy, Coulomb energy and specific energy, respectively. Further details of ReaxFF are shown in Ref. [26].

2.2. Case set-ups

The initial parameters of the simulated systems are shown in Table 1. In each case, the computational domain is a periodic box. System 1 contains 20 pyridine molecules only. In systems 2 to 8, there are 20−500H_2O molecules added to investigate the effects of water on pyridine pyrolysis. Fig. 1 shows the model configurations for pyridine pyrolysis without and with water. α is the ratio of the number of water molecules, n (H_2O), to the number of pyridine molecules, n (C_5H_5N), as shown in Equation (2). The density of each system is kept the same at 0.3 g/cm^3 by varying the size of the computational box.

$$\alpha = \frac{n(H_2O)}{n(C_5H_5N)} \quad (2)$$

2.3. Simulation details

In this paper, the Large-scale Atomic/Molecular Massively Parallel Simulator (LAMMPS) was used to carry out ReaxFF MD simulations of pyridine pyrolysis. The reactive force field of the C/H/O/N system was chosen, whose parameters are trained with quantum chemistry calculations and have been carefully validated [27,28]. The time step was 0.1 fs and the bond order cutoff value was 0.3. The NVT ensemble [29] was selected for all simulations. Due to excessive computational cost, MD typically adopts higher temperatures than in the experiments in order to accelerate simulations. This approach has been verified to reproduce reaction mechanisms observed in experiments [30–32].

Before "production" simulations, energy minimization and system equilibration were carried out. The temperature was kept constant at 1000 K for 50 ps After that, the temperature of each system is increased to a final temperature of 3000 K with a heating rate of 100 K/ps and then kept constant. The total simulation time is 1000 ps Three replicates with different initial positions of reactants were simulated for every case. The simulation was complemented via REAXC package on the platform of Large-scale Atomic/Molecular Massively Parallel Simulator (LAMMPS).

2.4. Post-processing

The reaction pathways are obtained by Chemical Trajectory AnalYzer (ChemTraYzer) scripts [33]. The dynamic trajectories were visualised using VMD [34]. Unless otherwise indicated, the data used in the figures of this study are the average results of the three replicate simulations. Error bars in all figures are Standard Error (SE) of three replicates.

Table 1
Initial parameters of the simulated systems.

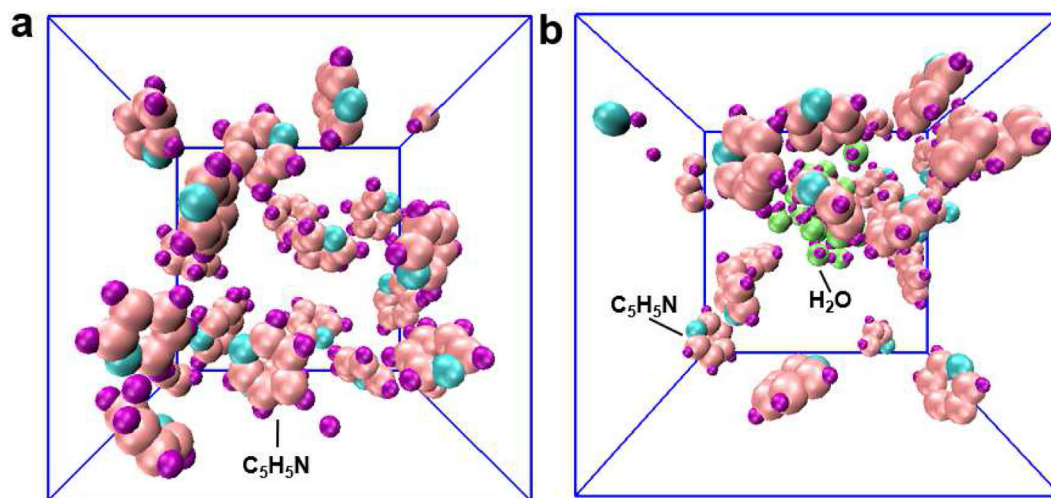| System	Number of C_5H_5N molecules	Number of H_2O molecules	α	Density (g/cm^3)	Box size(Å)
1	20	0	0	0.3	20.6118
2	20	20	1	0.3	22.0708
3	20	40	2	0.3	23.3588
4	20	60	3	0.3	24.5186
5	20	80	4	0.3	25.5780
6	20	100	5	0.3	26.5562
7	20	200	10	0.3	30.6168
8	20	500	25	0.3	38.8450

Fig. 1. Initial configurations for pyridine pyrolysis. (a) α = 0 (b) α = 1.
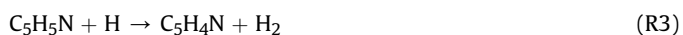
3. Results and discussions

3.1. Validation of simulations

The validation of the ReaxFF MD simulations is achieved by comparing intermediate products obtained from this study with those from previous studies. The key intermediate species are HCN, CN, NH$_3$, H$_2$ and C$_2$H$_2$, which agrees with previous work [30].

The mechanisms of pyridine pyrolysis and chemical effects of water during pyridine pyrolysis are analyzed in the following sections.

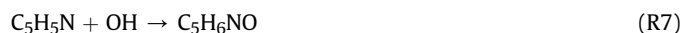## 3.2. Effects of water on pyridine consumption rate

Fig. 2a and b shows the time evolutions of C$_5$H$_5$N with α value ranging from 0 to 25 at 3000 K. At the initial stage up to 600 ps, at least 90% of C$_5$H$_5$N molecules are consumed in all cases. To study the water influence on consumption rate of pyridine, the consumption number of pyridine at different stages was calculated as shown in Fig. 2c. It is clear that water promotes pyridine consumption rate during the first 200 ps A similar phenomenon was also observed in previous studies that water can promote reactions during ethanol and methane oxidation and pyrolysis char [7,31,35]. Under water-free conditions, pyridine molecules are consumed by reactions:

$$C_5H_5N + H \rightarrow C_5H_6N \tag{R1}$$

$$C_5H_5N \rightarrow C_5H_4N + H \tag{R2}$$

$$C_5H_5N + H \rightarrow C_5H_4N + H_2 \tag{R3}$$

However, OH radicals are generated with water addition during pyridine pyrolysis by reactions:

$$H_2O \rightarrow OH + H \tag{R4}$$

$$H_2O + H \rightarrow OH + H_2 \tag{R5}$$

And new reactions are found during pyridine pyrolysis with water as follows:

$$C_5H_5N + OH \rightarrow H_2O + C_5H_4N \tag{R6}$$

$$C_5H_5N + OH \rightarrow C_5H_6NO \tag{R7}$$

The addition of water during the pyridine pyrolysis process brings OH radicals in the system and accelerates the consumption of pyridine. More details about the effects of water on intermediates are shown in Table 2, which will be discussed in Section 3.3. However, as the pyrolysis goes on, water presents obvious inhibitory effects on the consumption of pyridine. To explain this phenomenon, we investigated the effects of water on polycondensation compounds in Section 3.4.

3.3. Effects of water on intermediates

Fig. 3a and b describe time evolution of the total species number for α ranging from 0 to 25. In general, the species number during pyrolysis increases to a peak value and then deceases in both cases. And the species number in this case with water is significantly higher than that without water during pyridine pyrolysis. This implies H$_2$O molecules take part in various intermediate reactions
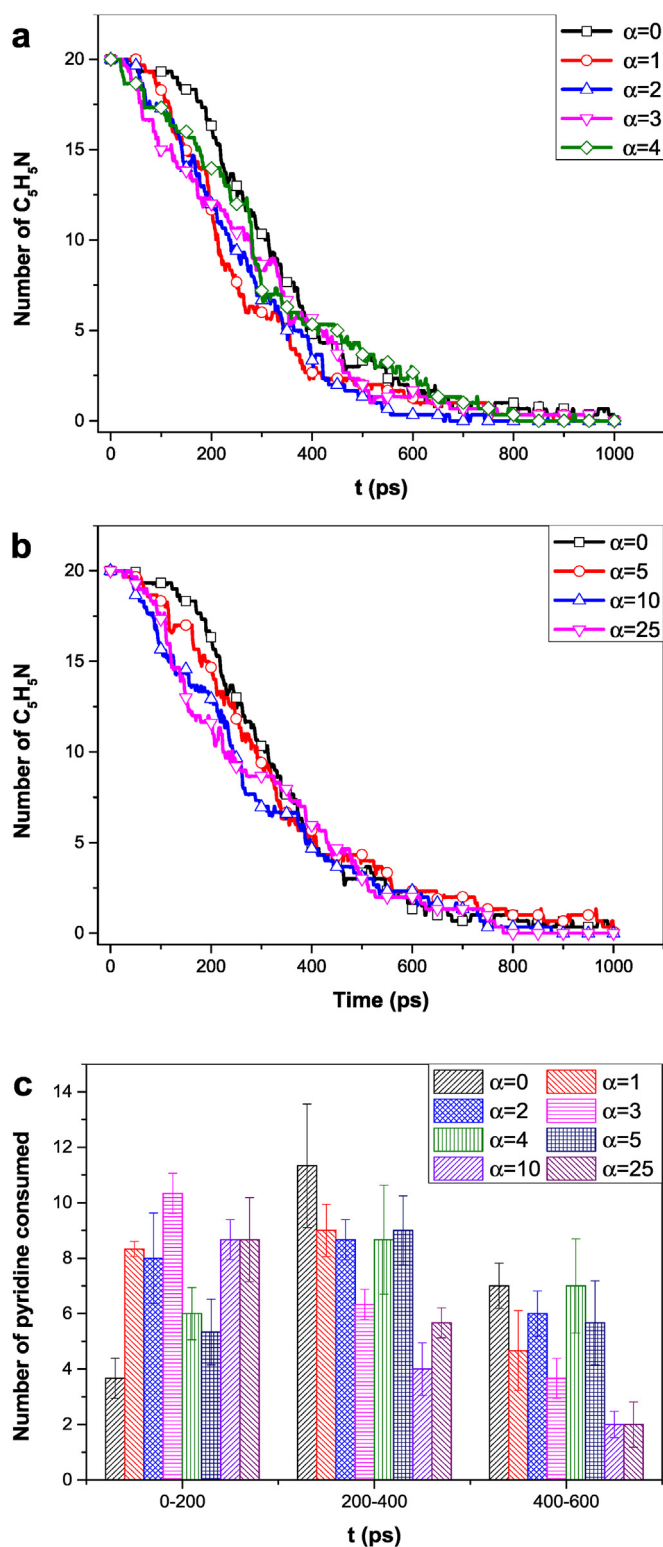
Fig. 2. Time evolution of C_5H_5N under varying α values and consumption number of pyridine at different stages. (a) $\alpha = 0-4$. (b) $\alpha = 0\&5-25$. (c) consumption number of pyridine.

Table 2
Main intermediates among cases with and without water addition. Different symbols are used to clarify the influence of water on intermediates. •: $\alpha = 0-25$, ◆: $\alpha = 1-25$, ♠: $\alpha = 2-25$, Δ: $\alpha = 4-25$, □: $\alpha = 5-25$, ×: $\alpha = 10-25$, ⊗: $\alpha = 3-5\&25$, ⊕: $\alpha = 4\&5\&25$, ♥: $\alpha = 5\&25$.

α	0	1	2	3	4	5	10	25
H_2	•	•	•	•	•	•	•	•
NH_3	•	•	•	•	•	•	•	•
CN	•	•	•	•	•	•	•	•
HCN	•	•	•	•	•	•	•	•
C_4H_2	•	•	•	•	•	•	•	•
C_4H_3	•	•	•	•	•	•	•	•
C_4H_4	•	•	•	•	•	•	•	•
CO		◆	◆	◆	◆	◆	◆	◆
CHNO		◆	◆	◆	◆	◆	◆	◆
CH_2NO		◆	◆	◆	◆	◆	◆	◆
C_2H_2O		◆	◆	◆	◆	◆	◆	◆
C_2H_3O		◆	◆	◆	◆	◆	◆	◆
CNO			♠	♠	♠	♠	♠	♠
CHO			♠	♠	♠	♠	♠	♠
CHO_2			♠	♠	♠	♠	♠	♠
C_2HO_2			♠	♠	♠	♠	♠	♠
CO_2					Δ	Δ	Δ	Δ
C_4H_3O						□	□	□
C_3H_4O							×	×
C_4H_4O							×	×
C_2O_2				⊗	⊗	⊗		⊗
C_3H_2O					⊕	⊕		⊕
C_3H_3O						♥		♥

is higher than 5, the number of species in the system remains more or less the same even with α increasing.

To further clarify the influence of water molecules on intermediates during pyridine pyrolysis, the intermediates are compared among cases under water-free and water conditions as shown in Table 2. H_2, NH_3, CN, HCN, C_4H_2, C_4H_3 and C_4H_4 are shared among all cases. CO, CHNO, CH_2NO, C_2H_2O and C_2H_3O are found in cases with water addition.

CNO, CHO, CHO_2 and C_2HO_2 are observed for α over $2-25$. CO_2 is produced in $\alpha = 4-25$ cases. C_4H_3O is spotted in cases with α of $5-25$. C_3H_4O and C_4H_4O are detected when α is 10 or 25. C_2O_2 occurs in $\alpha = 3, 4, 5$ and 25 cases. C_3H_2O and C_3H_3O are found in $\alpha = 4, 5, 25$ and $\alpha = 5, 25$ cases, respectively.

3.4. Effects of water on polycondensation compounds

During coal pyrolysis, there are both decomposition and polycondensation reactions. The pyrolysis products are char ($C_{40}+$), tar (C_5-C_{40}) and gas (C_0-C_5) in descending order according to the number of C atoms [13]. In this part, water influence on decomposition and polycondensation reactions is explored during pyridine pyrolysis.

Fig. 4a−c presents the proportion of C, N and H elements in C_5+ during pyridine pyrolysis. With the increase of water molecules in system, the percentages of C, N and H in C_5+ decrease greatly. When α is 25, few C_5+ compounds are formed during pyridine pyrolysis. This phenomenon is in agreement with previous experimental studies [7,8]. Results show that water molecules greatly inhibit polycondensation reactions and modify pathways to char, tar and gas, which is of great significance to control nitrogen migration during coal pyrolysis. In addition, according to the products analysis of pyridine in the water-free condition, the polycondensation reaction mainly occurs after 200 ps. This provides an explanation for the finding in Section 3.2 that water exerts obvious inhibitory effects on the consumption of pyridine after 200 ps. Fig. 4d shows snapshots of C_5+ with the increasing α. As the value of α ranges from 0 to 10, the number of C atoms contained in the polycondensation product is significantly reduced (from C_{21} to

and generate additional intermediates during the pyrolysis process. This result is also confirmed by results in Section 3.2 that water molecules produce OH radicals during pyridine pyrolysis, which promote the consumption of pyridine. Besides, when the value of α
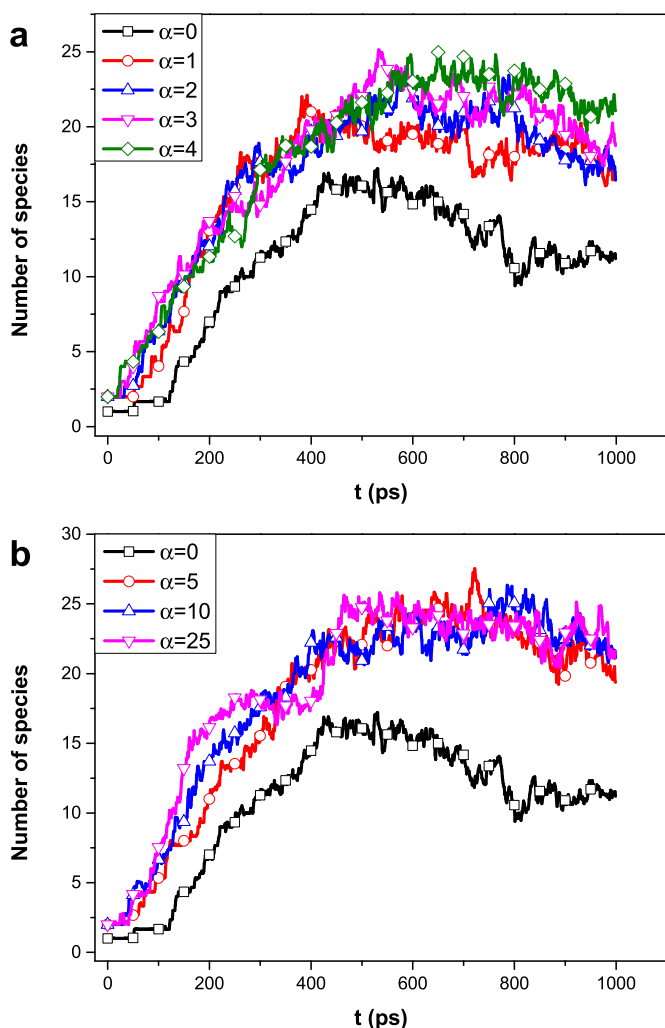
Fig. 3. Time evolution of the total species number under varying α values. (a) $\alpha = 0-4$. (b) $\alpha = 0\&5-25$.
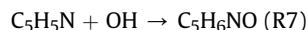
C_6). Besides, the increase of water molecules also promotes the existence of O atom in polycondensation products.

3.5. Effects of water on ring-opening reactions

According to previous studies [8,9], pyridine molecules undergo ring opening reactions firstly during pyrolysis. Fig. 5a illustrates snapshots of ring-opening reactions during pyridine pyrolysis at all cases. Four types of ring-opening pathways were detected by MD during pyridine pyrolysis. Type A happens when o-C_5H_5N reacts with H atom forming o-C_5H_6N firstly. Then o-C_5H_6N opens the ring to form a chain C_5H_6N. Type B occurs when C_5H_5N directly opens the ring to generate chain C_5H_5N. Type C is the case when pyridine molecules lose an H atom and then undergoes a ring-opening reaction, which is in agreement with previous studies [31,36−38]. Type D occurs when C_5H_5N reacts with OH radicals in the system to form an oxygen-containing intermediate and then ring-opening reaction occurs. As it happens, the H atom on the C atom adjacent to N atom is transferred to the N in all types. After that, chain intermediates (C_5) are pyrolyzed and HCN, CN, C_4H_4 and C_4H_3 are generated. The effects of water on key species will be discussed in detail in Section 3.6.

Fig. 5b shows the proportion of each type under different α values. As the content of water molecules in the system increases,

the proportion of pyridine molecules to open rings through type A and type B decreases. Besides, the percentage of type C increases to the peak point at $\alpha = 10$ and then decreases with increasing value of α. Ring-opening reactions of type D only occurs when the water content in the system is high. In pyridine pyrolysis without water addition, pyridine molecules convert to C_5H_6N and C_5H_4N through R1 to R3. The water addition brings about OH radical by reactions R4 and R5. And the OH radical promotes the generation of C_5H_4N by R6. Thus, water suppresses the ring-opening reactions via type A and type B and promotes type C of ring-opening reactions. However, when the value of α increases to 4, there are pathways to generate oxygen-containing intermediates (C_5H_6NO, C_5H_5NO, C_5H_4NO and C_5H_3NO). Those are:

$$C_5H_5N + OH \rightarrow C_5H_6NO \quad (R7)$$

$$C_5H_4N + H_2O \rightarrow C_5H_6NO \quad (R8)$$

$$C_5H_4N + H_2O \rightarrow C_5H_5NO + H \quad (R9)$$

$$C_5H_4N + HO \rightarrow C_5H_5NO \quad (R10)$$

$$C_5H_6NO \rightarrow C_5H_5NO + H \quad (R11)$$

$$C_5H_5NO + HO \rightarrow H_2O + C_5H_4NO \quad (R12)$$

$$C_5H_4NO \rightarrow C_5H_3NO + H \quad (R13)$$

Results indicate that H_2O accelerates the consumption of C_5H_4N and promotes the production of oxygen-containing intermediates. That is the reason why high concentration of water has an inhibitory effect on type C and type D only occurs in systems with high water concentration.

3.6. Effects of water on products H_2, CO, HCN and NH_3

Pyridine molecules undergo ring-opening reactions and then pyrolyze to produce the main intermediates HCN, CN, C_4H_4 and C_4H_3, which is in agreement with previous results [31,36−38]. In this part, we explore the effects of water on those radicals as well as principal products H_2, NH_3 and CO during pyridine pyrolysis.

Fig. 6 presents the effects of H_2O on the generation of H_2, CO, HCN and NH_3. As the number of H_2O molecules increases, the yield of H_2, CO and NH_3 shows an upward trend, which is in good agreement with a previous study in Ref. [6]. However, water influence on HCN is more complicated. When the value of α is in the range of 0−3, the yield of HCN remains the same. As α increases, a parabolic profile is observed which peaks at $\alpha = 10$. According to the findings in Section 3.4, water reduces the content of C, H and N in C_5+, which accounts for the increasing trend of H_2, CO and NH_3. To understand the trend of HCN, the influence of water on transfer pathways of main intermediates was interrogated as shown in Fig. 7a and b.

In pyridine pyrolysis under water-free conditions, H_2 mainly comes from H in the pyrolysis process, that is

$$H + H \rightarrow H_2 \quad (R14)$$

Water during the pyrolysis process adds a new pathway to H_2 by R5. Fig. 6a describes effects of H_2O on transfer pathways of nitrogen-containing intermediates. As pyrolysis goes on, HCN and CN will convert to NH_3 in all cases [30]. And the transfer pathway is HCN → CNH → NH → NH_2 → NH_3 [39]. However, due to the conversion of HCN and CN to N_2 occurring at high temperatures [30], N_2 is not observed in our simulations. New pathways HCN →
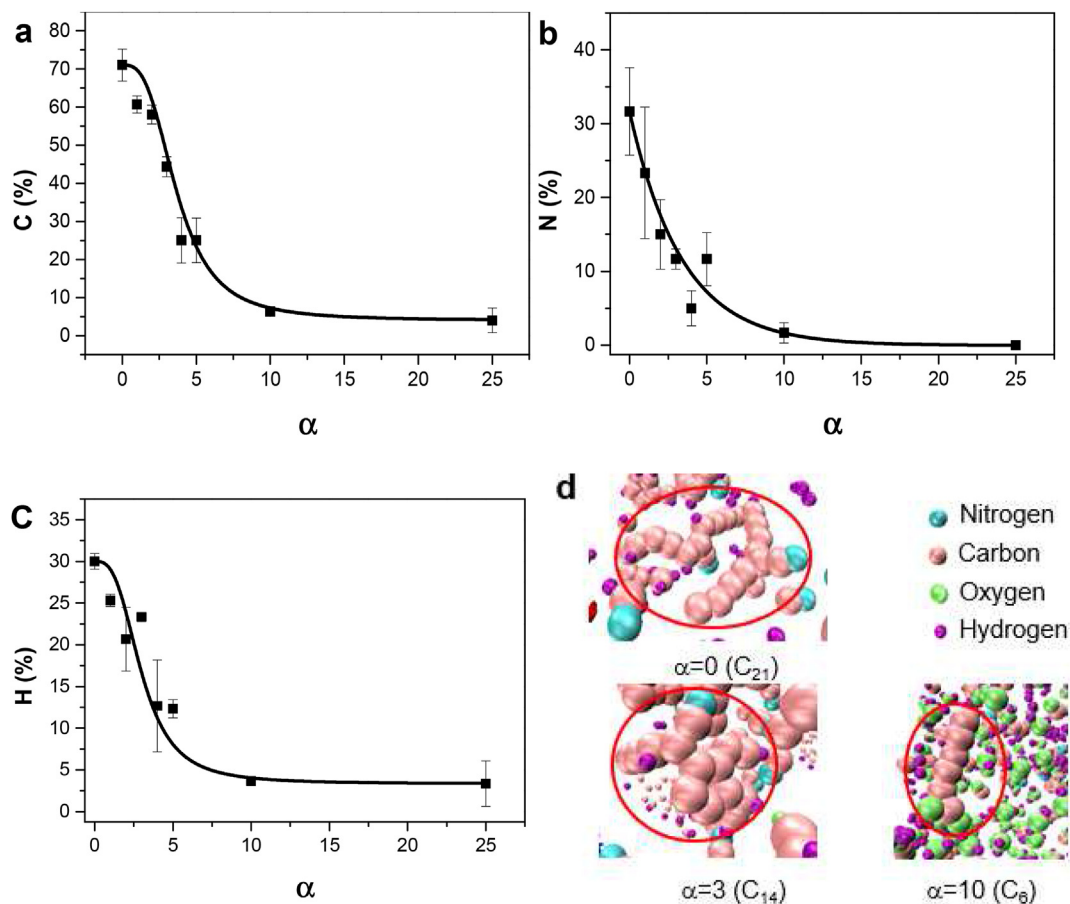
Fig. 4. The proportion of each element in C_5+ and snapshots of C_5+ under varying α values. (a) C; (b) N; (c) H; (d) snapshots of C_5+.

CH_2NO and $CH_2NO \rightarrow CHNO$ are generated with water addition during pyridine pyrolysis by reactions:

$$HCN + OH \rightarrow CH_2NO \tag{R15}$$

$$CH_2NO \rightarrow CHNO + H \tag{R16}$$

When α is greater than 2, R17 to R20 are found during the pyrolysis process as shown below:

$$CN + OH \rightarrow CHNO \tag{R17}$$

$$CN + H_2O \rightarrow CHNO + H \tag{R18}$$

$$CHNO \rightarrow CNO + H \tag{R19}$$

$$CH_2NO \rightarrow NH_2 + CO \tag{R20}$$

Besides, R21 takes place in the range of $\alpha = 4-25$ as follows:

$$CHNO \rightarrow CO + NH \tag{R21}$$

Combining the findings from Fig. 6c and d, it is clear that the influence of OH radicals on HCN dominates when the value of α is 0, 1 and 25. Thus, water shows an inhibitory effect on the yield of HCN in those cases. And due to the promotional effects on pyridine pyrolysis, water enhances HCN production over $\alpha = 2-10$. Besides, OH radicals add new pathways of NH and NH_2, which are important precursors to NH_3. H_2O also enhances the conversion of NH_2 to NH_3

via reaction:

$$H_2O + NH_2 \rightarrow NH_3 + HO \tag{R22}$$

Therefore, the yield of NH_3 is promoted with water addition during pyridine pyrolysis.

Fig. 7b describes water influence on migration pathways of main nitrogen-free intermediates during pyridine pyrolysis. In all cases, C_4H_4 and C_4H_3 were major initial nitrogen-free species during pyridine pyrolysis [30]. And C_2H_2 and C_2H are mainly produced by thermal decomposition of C_4H_4 and C_4H_3. C_4H_2 is formed by the loss of one H atom from C_4H_3. In pyridine pyrolysis with water addition, OH reacts with main intermediates (C_4H_3, C_4H_2, C_2H_2 and C_2H) to form CO. However, there are huge differences in transfer pathways to generating CO at various α values. When the H_2O content in the system is low (the value of α in the range 1–4), OH radicals mainly react with C_2 compounds to generate oxygen-containing intermediates by reactions:

$$C_2H + OH \rightarrow C_2H_2O \tag{R23}$$

$$C_2H_2 + OH \rightarrow C_2H_3O \tag{R24}$$
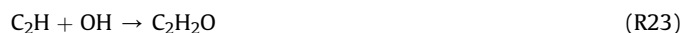
And C_2H_3O, C_2H_2O and CHO are key precursors forming CO for α ranging from 1 to 4. When the range of α is 2–25, CO will convert to CHO_2 through R25:
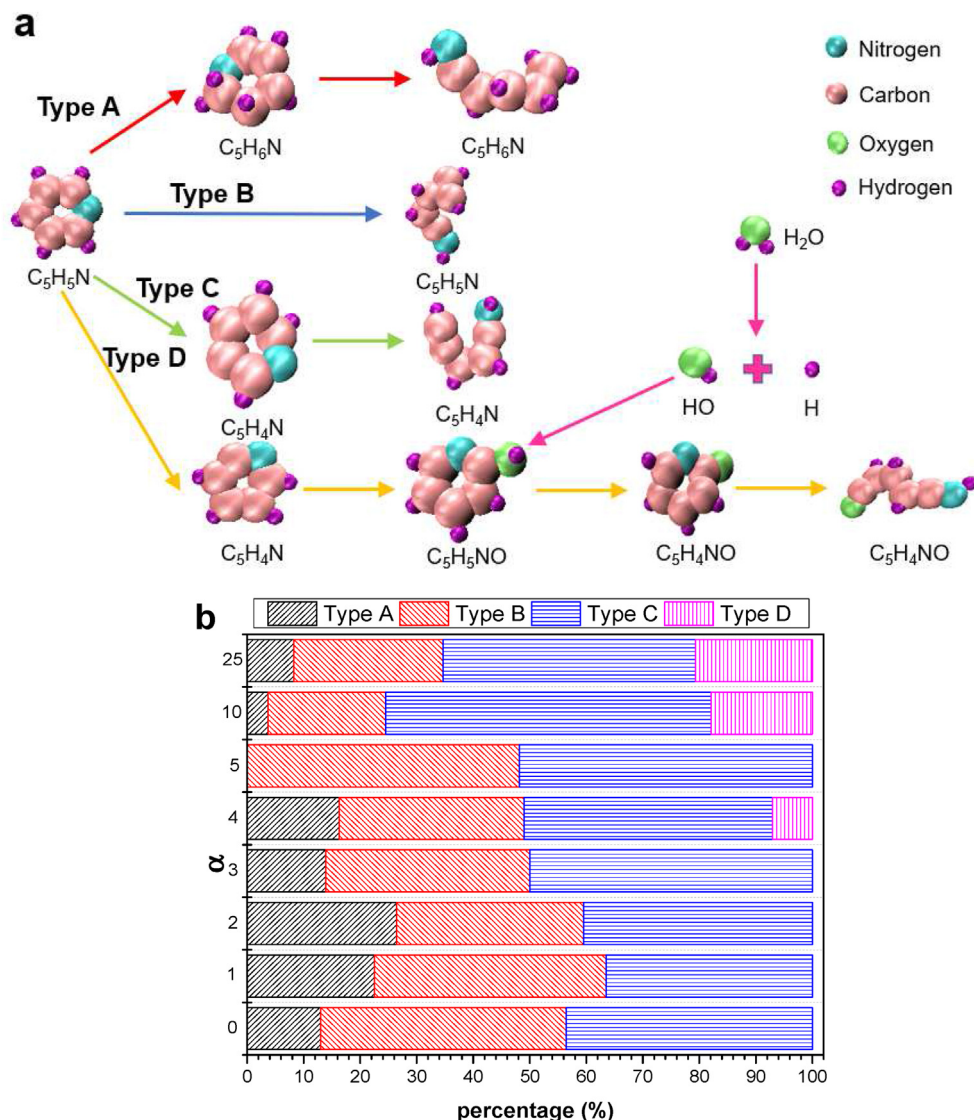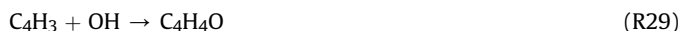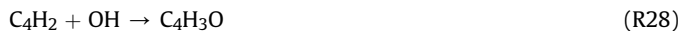
$$CO + OH \rightarrow CHO_2 \tag{R25}$$

Fig. 5. Schematic diagram of pyridine ring-opening reactions and the influence of on the types of ring-opening reactions. (a) Snapshots of four different types of pyridine ring-opening. (b) percentages of each type under varying .

And CO_2 is generated by decomposition of CHO_2 through R26 with $\alpha = 4-25$.

$$CHO_2 \rightarrow CO_2 + H \tag{R26}$$

When the value of α is $5-25$, OH radicals will react with C_3&C_4 compounds via reactions:

$$C_3H_3 + OH \rightarrow C_3H_4O \tag{R27}$$

$$C_4H_2 + OH \rightarrow C_4H_3O \tag{R28}$$

$$C_4H_3 + OH \rightarrow C_4H_4O \tag{R29}$$

And C_4H_2O, C_4H_3O, C_3H_3O, C_3H_2O and C_2O_2 are key intermediates to form CO. In addition, the pathway $HCN \rightarrow CH_2NO \rightarrow CO$ is broadly shared in water addition cases.

4. Discussion

In the present study, ReaxFF MD simulations were conducted to understand the influence of water on nitrogen-containing compounds (pyridine) in coal pyrolysis. We have uncovered new intermediates and reaction pathways that were not reported in previous studies [6,9]. Besides, the effects of water molecules on the consumption rate of pyridine and ring opening processes of pyridine molecules are also revealed at the atomic level. Based on the aforementioned analysis, we have demonstrated that the modification of pyrolysis by water addition can be applied to improve NOx control performance in the fuel splitting and staging process.

In the fuel splitting and staging process, the released nitrogen-containing species from large N-containing compounds are beneficial for NOx reduction as it can reduce nitrogen oxides selectively [4,5,40]. However, Greul et al. also proposed that small N-
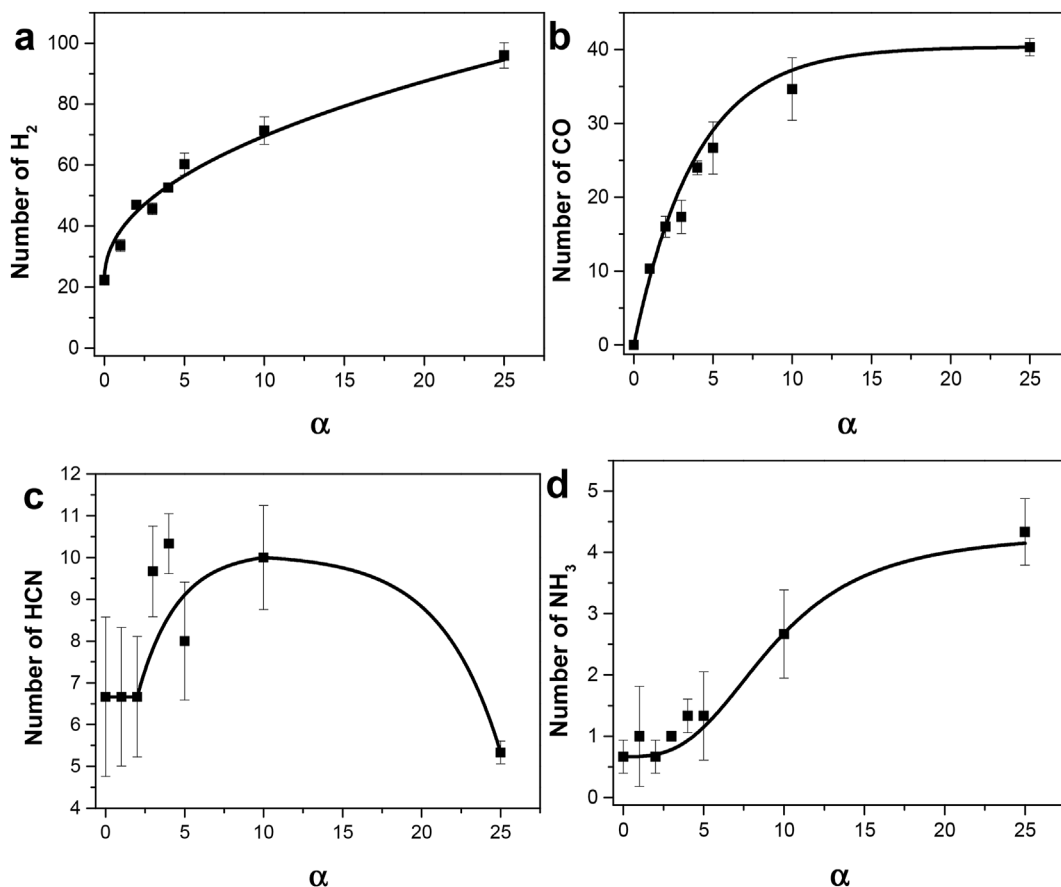
Fig. 6. Effects of H_2O on the yield of main products. (a) H_2. (b) CO. (c) HCN. (d) NH_3.

containing species in pyrolysis gas will react with O_2 to form NOx, causing negative impact on NOx control [40]. Hence, controlling the proportion of large *N*-containing compounds in the pyrolysis gas and the pyrolysis process of *N*-containing compounds is important to reduce NOx emissions. The current results suggest that the addition of water molecules would modify the reaction pathways in the pyrolysis process of *N*-containing compounds, thus achieving maximum NOx reduction.

Though nitrogen-containing compounds show better NOx reduction performance than nitrogen-free compounds, nitrogen-free radicals can also convert NOx to N_2. According to previous studies [41,42], the possibility of non-hydrocarbon fuels, such as H_2 and CO, to reduce NO to N_2 is low compared with the hydrocarbon radicals in the reburning process. According to the present research, the addition of water can promote conversion of hydrocarbon compounds to small *C*-containing radicals, which is beneficial for NOx control. On the other hand, high water concentration will convert hydrocarbon compounds into CO, CO_2 and H_2, alleviating NOx reduction in the reburning process. Thus, a proper water content in the process of reburning is required if water is used to regulate NO generation.

In general, the regulating effects of water on pyridine pyrolysis is monotonic. This behaviour is beneficial for control of the pyrolysis process. However, there are also non-monotonic behaviors with respect to water content in intermediate species (C_2O_2, C_3H_2O and C_3H_3O) and consumption rates of pyridine pyrolysis. For

intermediate species C_2O_2, C_3H_2O and C_3H_3O, when the value of α is lower than 10, the process is controlled by the condensation reaction of species (CO reacts with CO, C_2H_2 and C_2H_3, respectively). It is found that the yields of C_2O_2, C_3H_2O and C_3H_3O are low, and their roles in the conversion of NOx to N_2 are insignificant [41,42]. Thus, their effects on NOx control can be neglected. The non-monotonic relationship between water content and pyridine consumption rates suggest that different strategies for NOx control are required as the reaction evolves at different stages.

5. Conclusions

In this study, pyridine pyrolysis without and with water were investigated via ReaxFF-MD simulations. The effects of the added water with different proportions on pyridine pyrolysis reactions were investigated in detail. It is found that the addition of water during the pyridine pyrolysis process facilitates the generation of OH radicals and accelerates the consumption of pyridine at the initial stage of pyrolysis. By contracts, as water greatly inhibits the condensation reaction of pyridine molecules, water exerts inhibitory effects on the consumption of pyridine as pyrolysis goes on. Furthermore, water has significant influence on the total number of species during the pyridine pyrolysis and intermediates are identified and quantified under various conditions. In addition, water also reduces the N content in the polycondensation product (C_5+). This research provides new insights into atomic-level mechanisms
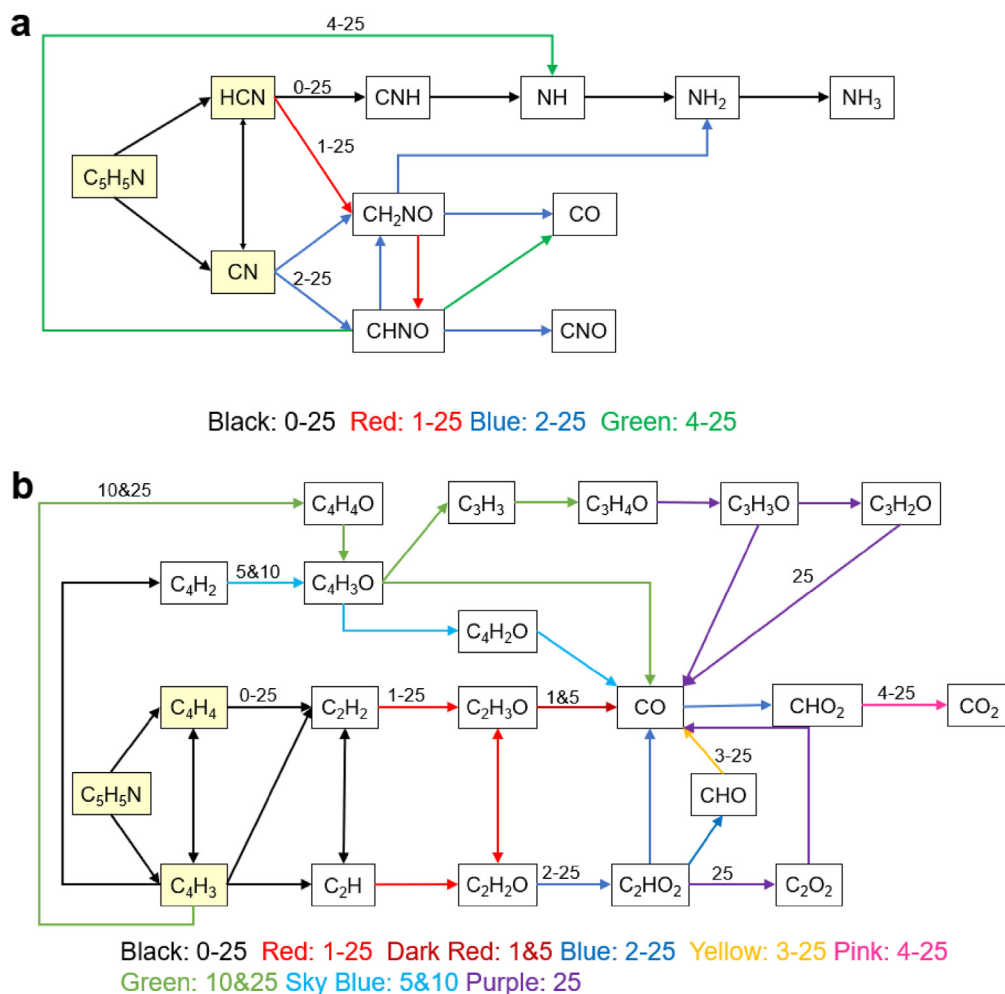
Fig. 7. Effects of H₂O on transfer pathways. (a) nitrogen-containing. (b) nitrogen-free intermediates. The numerical values in the figure are values of α. The species in the yellow box are the starting intermediates. (For interpretation of the references to colour in this figure legend, the reader is referred to the Web version of this article.)

of pyridine pyrolysis under water and water-free conditions, and has implications on control of N migration during the pyrolysis process and the emission of nitrogenous pollutants from coal pyrolysis and combustion.

Declaration of competing interest

The authors declare that they have no known competing financial interests or personal relationships that could have appeared to influence the work reported in this paper.

Acknowledgements

References

[1] Bowman CT. Control of combustion-generated nitrogen oxide emissions: technology driven by regulation. Symposium (International) on Combustion 1992;24(1):859−78.
[2] Luan T, Wang X, Hao Y, Cheng L. Control of NO emission during coal reburning. Appl Energy 2009;86(9):1783−7.
[3] Greul USH, Magel H-C, Schnell U, Rüdiger H, Hein K. Impact of temperature and fuel-nitrogen content on fuel-staged combustion with coal pyrolysis gas. Symposium (International) on Combustion 1996;26:2231−9.
[4] Rüdiger H, Greul U, Spliethoff H, Hein KR. Distribution of fuel nitrogen in pyrolysis products used for reburning. Fuel 1997;76(3):201−5.
[5] Rüdiger H, Kicherer A, Greul U, Spliethoff H, Hein K. Pyrolysis gas from biomass and pulverized biomass as reburn fuels in staged coal combustion. Developments in thermochemical biomass conversion. Springer; 1997. p. 1387−98.
[6] Gou X, Zhou J, Liu J, Cen K. Effects of water vapor on the pyrolysis products of pulverized coal. Procedia Environmental Sciences 2012;12:400−7.
[7] Ouyang J, Hong D, Jiang L, Li Z, Liu H, Luo G, et al. Effect of CO₂ and H₂O on char properties. Part 1: pyrolysis char structure and reactivity. Energy Fuels 2020;34(4):4243−50.
[8] Hu E, Zeng X, Ma D, Wang F, Yi X, Li Y, et al. Effect of the moisture content in coal on the pyrolysis behavior in an indirectly heated fixed-bed reactor with internals. Energy Fuels 2017;31(2):1347−54.
[9] Liu J, Lu Q, Jiang X-y, Hu B, Zhang X-l, Dong C-q, et al. Theoretical investigation of the formation mechanism of NH₃ and HCN during pyrrole pyrolysis: the

effect of H₂O. Molecules 2018;23(4):711.

[10] Jiang XZ, Luo KH, Ventikos Y. Principal mode of Syndecan-4 mechano-transduction for the endothelial glycocalyx is a scissor-like dimer motion. Acta Physiol 2020;228(3):e13376.

[11] Jiang XZ, Feng M, Zeng W, Luo KH. Study of mechanisms for electric field effects on ethanol oxidation via reactive force field molecular dynamics. Proc Combust Inst 2019;37(4):5525−35.

[12] Jiang XZ, Luo KH. Reactive and electron force field molecular dynamics simulations of electric field assisted ethanol oxidation reactions. Proc Combust Inst 2021;38(4):6605−13.

[13] Zheng M, Li X, Liu J, Guo L. Initial chemical reaction simulation of coal pyrolysis via ReaxFF molecular dynamics. Energy Fuels 2013;27(6):2942−51.

[14] Bhoi S, Banerjee T, Mohanty K. Molecular dynamic simulation of spontaneous combustion and pyrolysis of brown coal using ReaxFF. Fuel 2014;136:326−33.

[15] Castro-Marcano F, Russo Jr MF, van Duin AC, Mathews JP. Pyrolysis of a large-scale molecular model for Illinois no. 6 coal using the ReaxFF reactive force field. J Anal Appl Pyrol 2014;109:79−89.

[16] Zheng M, Li X, Liu J, Wang Z, Gong X, Guo L, et al. Pyrolysis of Liulin coal simulated by GPU-based ReaxFF MD with cheminformatics analysis. Energy Fuels 2014;28(1):522−34.

[17] Chen B, Diao Z-J, Zhao Y-L, Ma X-X. A ReaxFF molecular dynamics (MD) simulation for the hydrogenation reaction with coal related model compounds. Fuel 2015;154:114−22.

[18] Li W, Zhu Y-m, Wang G, Wang Y, Liu Y. Molecular model and ReaxFF molecular dynamics simulation of coal vitrinite pyrolysis. J Mol Model 2015;21(8):188.

[19] Chenoweth K, Van Duin AC, Goddard WA. ReaxFF reactive force field for molecular dynamics simulations of hydrocarbon oxidation. J Phys Chem 2008;112(5):1040−53.

[20] Han S-p, van Duin AC, Goddard III WA, Strachan A. Thermal decomposition of condensed-phase nitromethane from molecular dynamics from ReaxFF reactive dynamics. J Phys Chem B 2011;115(20):6534−40.

[21] Strachan A, Kober EM, van Duin AC, Oxgaard J, Goddard III WA. Thermal decomposition of RDX from reactive molecular dynamics. J Chem Phys 2005;122(5):054502.

[22] Wang Ca, Du Y, Jin X, Che D. Pyridine and pyrrole oxidation under oxy-fuel conditions. Energy Sources, Part A Recovery, Util Environ Eff 2016;38(7):975−81.

[23] Solomon PR, Colket MB. Evolution of fuel nitrogen in coal devolatilization. Fuel 1978;57(12):749−55.

[24] Nelson PF, Kelly MD, Wornat MJ. Conversion of fuel nitrogen in coal volatiles to NOx precursors under rapid heating conditions. Fuel 1991;70(3):403−7.

[25] Van Duin AC, Dasgupta S, Lorant F, Goddard WA. ReaxFF: a reactive force field for hydrocarbons. J Phys Chem 2001;105(41):9396−409.

[26] Senftle TP, Hong S, Islam MM, Kylasa SB, Zheng Y, Shin YK, et al. The ReaxFF reactive force-field: development, applications and future directions. npj Computational Materials 2016;2(1):1−14.

[27] Zhang L, Duin ACv, Zybin SV, Goddard Iii WA. Thermal decomposition of hydrazines from reactive dynamics using the ReaxFF reactive force field. J Phys Chem B 2009;113(31):10770−8.

[28] Zhang L, Zybin SV, Van Duin AC, Dasgupta S, Goddard III WA, Kober EM. Carbon cluster formation during thermal decomposition of octahydro-1, 3, 5, 7-tetranitro-1, 3, 5, 7-tetrazocine and 1, 3, 5-triamino-2, 4, 6-trinitrobenzene high explosives from ReaxFF reactive molecular dynamics simulations. J Phys Chem 2009;113(40):10619−40.

[29] Andersen HC. Molecular dynamics simulations at constant pressure and/or temperature. J Chem Phys 1980;72(4):2384−93.

[30] Liu J, Guo X. ReaxFF molecular dynamics simulation of pyrolysis and combustion of pyridine. Fuel Process Technol 2017;161:107−15.

[31] Feng M, Jiang XZ, Zeng W, Luo KH, Hellier P. Ethanol oxidation with high water content: a reactive molecular dynamics simulation study. Fuel 2019;235:515−21.

[32] Hong D, Li P, Si T, Guo X. ReaxFF simulations of the synergistic effect mechanisms during co-pyrolysis of coal and polyethylene/polystyrene. Energy 2021;218:119553.

[33] Döntgen M, Przybylski-Freund M-D, Kröger LC, Kopp WA, Ismail AE, Leonhard K. Automated discovery of reaction pathways, rate constants, and transition states using reactive molecular dynamics simulations. J Chem Theor Comput 2015;11(6):2517−24.

[34] Humphrey W, Dalke A, Schulten K. VMD: visual molecular dynamics. J Mol Graph 1996;14(1):33−8.

[35] Hong D, Liu L, Huang Y, Zheng C, Guo X. Chemical effect of H₂O on CH₄ oxidation during combustion in O₂/H₂O environments. Energy Fuels 2016;30(10):8491−8.

[36] Mackie JC, Colket MB, Nelson PF. Shock tube pyrolysis of pyridine. J Phys Chem 1990;94(10):4099−106.

[37] Hore N, Russell D. Radical pathways in the thermal decomposition of pyridine and diazines: a laser pyrolysis and semi-empirical study. Journal of the Chemical Society, Perkin Transactions 1998;2(2):269−76.

[38] Memon H, Bartle K, Taylor J, Williams A. The shock tube pyrolysis of pyridine. Int J Energy Res 2000;24(13):1141−59.

[39] Luo J, Zou C, He Y, Jing H, Cheng S. The characteristics and mechanism of NO formation during pyridine oxidation in O₂/N₂ and O₂/CO₂ atmospheres. Energy 2019;187:115954.

[40] Impact of temperature and fuel-nitrogen content on fuel-staged combustion with coal pyrolysis gas. In: Greul U, Spliethoff H, Magel H-C, Schnell U, Rüdiger H, Hein K, et al., editors. Symposium (international) on combustion. Elsevier; 1996.

[41] Dagaut P, Lecomte F. Experiments and kinetic modeling study of NO-reburning by gases from biomass pyrolysis in a JSR. Energy Fuels 2003;17(3):608−13.

[42] Glarborg P, Kristensen PG, Dam-Johansen K, Alzueta M, Millera A, Bilbao R. Nitric oxide reduction by non-hydrocarbon fuels. Implications for reburning with gasification gases. Energy Fuels 2000;14(4):828−38.